

Polarization Rotating Mach Zehnder Interferometer Based on Si Waveguide Platform

Yosuke Onawa¹, H. Okayama¹, and D. Shimura, *Member, IEEE*

Abstract—Polarization rotating (PR) Mach Zehnder Interferometer (MZI) device is proposed based on Si waveguide platform using multimode concept and experimentally demonstrated. Its concept is to use the mode conversion between TE first order and TM fundamental modes. The device is composed of mode converters, multimode directional couplers and PR rib waveguides inserted to the center of each arm waveguide. Fabricated PR MZI device shows good matching in the spectra between TE and TM polarizations in terms of the operation wavelength and the device loss.

Index Terms—Mach Zehnder interferometer, multimode, polarization independent, silicon photonics, waveguide device, wavelength division multiplexing.

I. INTRODUCTION

BECAUSE of the advent of 5G mobile and IoT, the demand for the large transmission capacity in the data center or access network has been enhanced, which makes wavelength division multiplexing (WDM) system an important solution to avoid inflating the infrastructure cost and the physical volume of the optical components. The optical transceivers need to be low cost and small enough to be placed everywhere inside the server racks or buildings.

Si photonics have been expected as a promising platform for optical transceivers due to its potential of integrating optical devices such as waveguides, WDM filters, modulators and photo detectors, and reducing the cost by the mass production with CMOS process. Furthermore, the optical circuit size can be shrunk by using the waveguide composed of Si core and SiO₂ clad with high refractive index contrast (Δ) [1], [2].

However, such high Δ waveguides tend to suffer from the polarization dependence. At the receiver side in the optical link, where random polarized signals come via optical fibers, such polarization dependence induces the polarization dependent loss (PDL) and crosstalk degradation arising from the difference of the transmission spectra between TE and TM polarizations.

Mach Zehnder Interferometer (MZI) is one of the well-known WDM devices because arbitrary spectrum characteristics can be obtained by combining several MZI devices

with various transmission spectra [3], [4]. As mentioned above, MZI devices used in the receiver side must be independent of light polarizations. Here, we define “polarization independent (PI)” as the condition in which WDM device passes or cuts the optical signals at the same wavelength and PDL is sufficiently suppressed between TE and TM polarizations.

Many researchers have dealt with this polarization issue by introducing the polarization diversity technique into the optical circuit [5], [6]. However, this method requires twice the number of the devices designed for each optical path and these devices should operate identically. Thus, optical circuits tend to be large and complex or require a precise fabrication process. We have proposed to make MZI device itself PI to simplify the optical circuit for WDM applications without using polarization diversity [7]. Reference [7], the combination of two arm waveguides is optimized to achieve PI condition for the optical phases by adjusting the relation between each width and length of two arm waveguides. However, dimensional errors of the waveguide determined by the process accuracy may lead to the optical phase mismatch, resulting in the mismatch of the wavelength responses between TE and TM polarizations.

In this letter, we propose PI MZI devices based on Si waveguide platform by utilizing mode conversion between TE first order mode (TE₁) and TM fundamental mode (TM₀), i.e. polarization rotating (PR) function. Because the phase difference between TE₁ and TM₀ at the arm waveguides can be canceled due to the mode complementary relationship of TE and TM polarizations, any arm design can be adapted as the phase shifters, which means the degree of achievement of “polarization independence” is not affected by the process error. Thus, identical wavelength responses can be guaranteed for both polarizations with single MZI device.

II. DEVICE STRUCTURE

Fig. 1 shows the schematic top view of PR MZI device. The device is composed of mode converters (Fig. 2 (a)), multimode directional couplers (MMDCs, Fig. 2 (b)), arm waveguides sandwiched by them and PR rib waveguides (Fig. 2 (c)) positioned on the center of each arm waveguide. Each mode converter is placed at the input and output sides. It exchanges TE fundamental mode (TE₀) for TE first order mode (TE₁), while having no effect on TM fundamental mode (TM₀). Thus, TE₁ and TM₀ pass through from the mode converter at the input side to those of output side.

Manuscript received 6 July 2022; revised 20 September 2022; accepted 29 September 2022. Date of publication 4 October 2022; date of current version 14 October 2022. (Corresponding author: Yosuke Onawa.)

The authors are with Oki Electric Industry Company Ltd., Warabi 335-8510, Japan (e-mail: oonawa834@oki.com; okayama575@oki.com; shimura273@oki.com).

Color versions of one or more figures in this letter are available at <https://doi.org/10.1109/LPT.2022.3211617>.

Digital Object Identifier 10.1109/LPT.2022.3211617

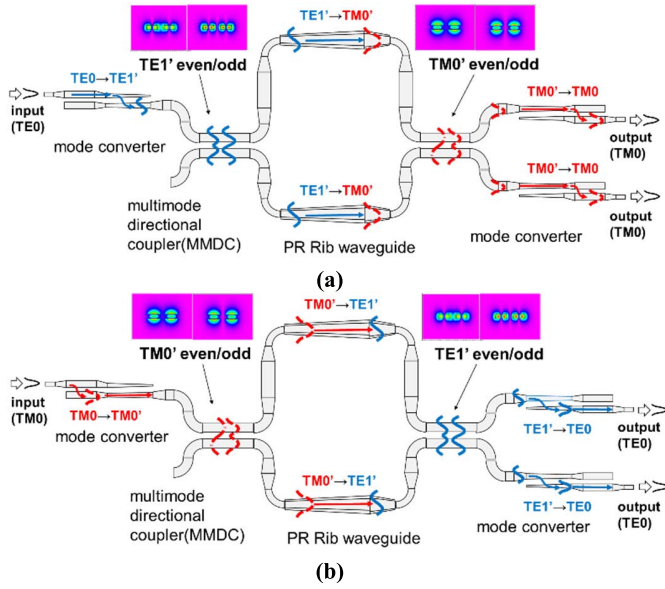


Fig. 1. Schematic top view of PR MZI device, illustrating how the beams propagate through the device, for the case of (a) TE0 input, (b) TM0 input respectively.

MMDCs are designed to have the same coupling strength between TE1 and TM0 by optimizing the waveguide dimensions, i.e. waveguide width, height and the gap between them. Its design concept is based on [7].

At the center region of each arm waveguide, the rib cross-sectional waveguides are inserted for the mode conversion between TE1 and TM0 modes. As the light traveling each arm waveguide goes through the same optical phase shift for TE1 and TM0, the phase difference between TE1 and TM0 can be compensated. At the output side, TE1 and TM0 modes are converted back to TE and TM fundamental modes by the mode converters, which means PR MZI device can be compatible with other single mode devices. We would present how to design each component forming PR MZI in the next section.

The mode converters are decomposed into two polarization beam splitters (PBS) connected in series as shown in Fig. 2(a). First one (PBS1) is a normal directional coupler with high aspect ratio (width / height) cross-section. In such directional coupler, the coupling strength of TM0 is much stronger than that of TE0. Thus, in PBS1, TM0 transits to the adjacent waveguide, while TE0 remains in the original waveguide. Second PBS (PBS2) is an asymmetrical directional coupler for the coupling between TE0 in the original waveguide and TE1 in the adjacent waveguide to which TM0 is already transited. Mode coupling condition between TE0 and TE1 is to satisfy below equation,

$$N_{TE0} = N'_{TE1} \quad (1)$$

Here, N_{TE0} and N'_{TE1} are the effective indices of TE0 in the original waveguide and TE1 in the adjacent waveguide. While no coupling occurs between TM0s in the original and the adjacent waveguides. To broaden the operation wavelength range of PBS2, each waveguide arranged in parallel has tapered width structure along to the propagating direction, in which effective index changes according to the width continuously. Detail parameters are summarized in Table I.

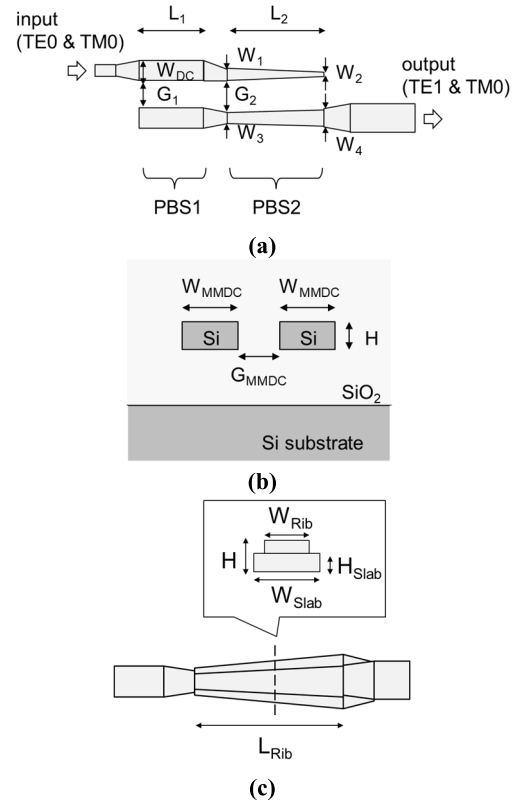


Fig. 2. (a) Top view of mode converter composed of PBS1 and PBS2, (b) cross-section of MMDC, (c) Top view of PR rib waveguide with its cross-section in the inset.

TABLE I
DESIGN PARAMETER OF MODE CONVERTER

	PBS1	PBS2	MMDC	PR-Rib
Height[nm]		H:220		(H _{Slab} :150)
Width[nm]	W_{DC} :600	W_1 :350 \rightarrow W_2 :100 W_3 :450 \rightarrow W_4 :550	W_{MMDC} :752	W_{Rib} :350 \rightarrow 800 W_{Slab} :550 \rightarrow 1000
Gap[nm]	G_1 :400	G_2 :500	G_{MMDC} :400	
Length[um]	L_1 :28	L_2 :100	L_{MMDC} :52	L_{Rib} :100

We verified the transmission spectrum of the designed mode converter by three dimensions finite differential time domain (3D-FDTD) simulation (Fig. 3). When TE0 mode is input into the mode converter, TE1 is output with the isolation about -20 dB against TE0 mode, which is critical for the device performance because TE0 could be the noise component.

While TM0 spectrum has its coupling characteristic as a directional coupler (PBS1) depending on the wavelength. The operating range of the mode converter is wide enough to cover C-band fully.

The MMDC (Fig. 2 (b)) was optimized to have equal coupling strength between TE1 and TM0 as a PI coupler. For that purpose, we adjusted the waveguide width (W_{MMDC}) and its gap (G_{MMDC}) as design parameters. Fig. 4 shows the relation between W_{MMDC} and the perfect coupling lengths of TE0, TE1 and TM0 with its gap fixed to 400 nm. At the cross point of each mode, the equal coupling strengths can be obtained for the corresponding modes. As can be seen, when W_{MMDC} is 752 nm, the coupling strengths get to be equal between TE1 and TM0 at the gap of 400 nm. Although the cross point for TE0 and TM0 is found at the width of

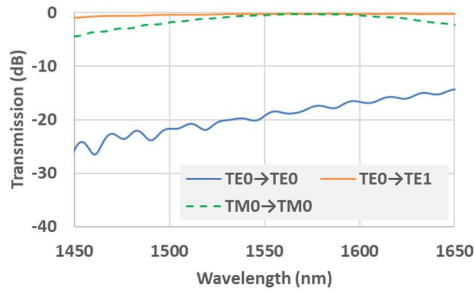


Fig. 3. Calculated spectrum of designed mode converter obtained by 3D-FDTD. Left side of arrow is input mode, while right side indicates output mode.

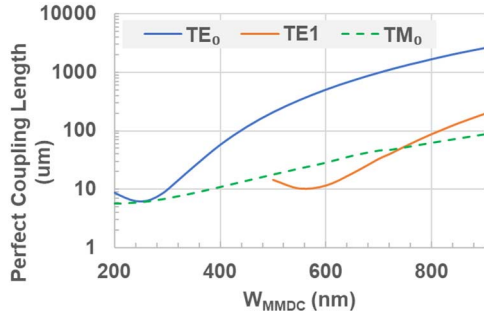


Fig. 4. The relation between W_{MMDC} and the perfect coupling length of TE0, TE1 and TM0 in MMDC. The gap is fixed to 400 nm.

260nm, such small cross-sectional waveguide results in the leakage mode, causing the leakage loss into the substrate or the bending loss at the curving waveguide. Thus, we set the W_{MMDC} to 752 nm and the coupling length (L_{MMDC}) to 52 μm as a 3 dB coupler (Table I).

The cross-section of the PR rib waveguide is shown in the inset of Fig. 2(c). The rib cross-section is employed for the asymmetric electric field toward the height direction to break the mode orthogonality between TE1 and TM0. The slab and rib widths are tapered along the propagating direction. In the rib waveguide, mode matching condition between TE1 and TM0 is defined as below,

$$N'_{RTE1} = N'_{RTM0} \quad (2)$$

Here, N'_{RTE1} and N'_{RTM0} represent the effective indices of TE1 and TM0 in the rib waveguide respectively. To do so, the rib and slab widths (W_{Rib} , W_{Slab}) vary from 350 nm to 800 nm and 550 to 1000 nm. The PR rib waveguide length (L_{Rib}) is set to 100 μm to obtain enough coupling strength between two modes. We verified the wavelength response of the designed PR rib waveguide by 3D-FDTD simulation. Fig. 5 shows the calculated transmission characteristics of each mode when TE1 is input into it. It can be seen when TE1 is input into the PR rib waveguide, it is converted to TM0 with the excess loss of about -0.5 dB. The isolation against original TE1 is suppressed below -15 dB and TE0 component as a noise is suppressed small enough to be neglected (smaller than -40 dB).

As a phase shifter, the arm waveguides can adopt any design parameter due to the PR effect in which the optical phase mismatch between TE1 and TM0 is compensated in the arm waveguides. It means even if the dimensional errors of the arm waveguides occur during the fabrication process, it is

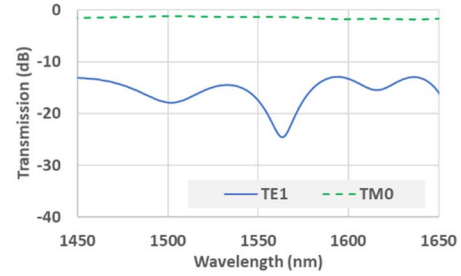


Fig. 5. Calculated transmission spectrum of PR rib waveguide by 3D-FDTD for the case of TE1 input.

guaranteed that the same wavelength response can be achieved between TE1 and TM0 as long as the PR effect occurs. The optical phase shifts for TE1 and TM0 at the arm waveguides are given equally by below equation ideally,

$$\phi = \frac{\pi}{\lambda} (N'_{ATE1} + N'_{ATM0})L \quad (3)$$

Here, N'_{ATE1} and N'_{ATM0} are the effective indices of TE1 and TM0 in the arm waveguide and L is length difference between upper and lower arm waveguides. We set arm waveguide width to 850 nm. At the bending regions, 580 nm-width multimode waveguide is used and bending radius is set to 20 μm to suppress unwanted mode conversion between TE1 and TE0 modes. Two PR MZI devices are designed to have different wavelength spacings of 26 nm and 13 nm for the purpose of verifying the operating principle of our PR device concept. All parameters for each component are summarized in Table I.

III. EXPERIMENTAL

The designed devices were fabricated by 300 mm SOI wafer process. Layer thicknesses are 220 nm for SOI layer and 3 μm for buried oxide layer respectively. The process included the photo lithography using the immersion ArF excimer laser ($\lambda = 193$ nm) and the dry etching to define the waveguide patterns. Then the patterned waveguides were covered by SiO_2 clad by chemical vapor deposition. Finally, the patterned wafer was diced into the chip by the dicing technology. Fig. 6 shows the photograph of fabricated PR MZI devices. Device size was about $600 \times 120 \mu\text{m}^2$, which was not much larger than that of single polarized device.

The measurement was conducted with the fiber alignment system using single mode fibers with lensed facet for the efficient coupling to the inverse tapered spot size converter (SSC) on the chip [8]. The super luminescent diode as a broad band light source sent the continuous wave to the device chip via the polarization controller and the received signal from the chip was collected by the same lensed fiber as input side and sent to the spectrum analyzer.

The device performance was defined as the transmission spectrum of the device patterned waveguide by subtracting that of the reference waveguide with the same length. The cross-section size of the reference waveguide was $440 \times 220 \text{ nm}^2$ to maintain the singlemode condition. We fabricated two PR MZI devices with different wavelength spacings of 26 nm and 13 nm.

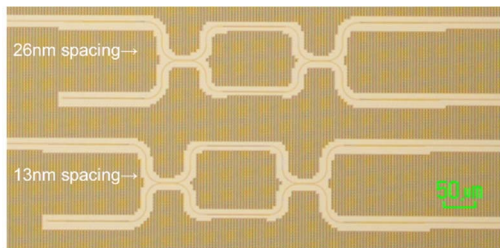


Fig. 6. Photograph of two fabricated PR MZI devices: upper for 26nm and bottom for 13nm wavelength spacing respectively.

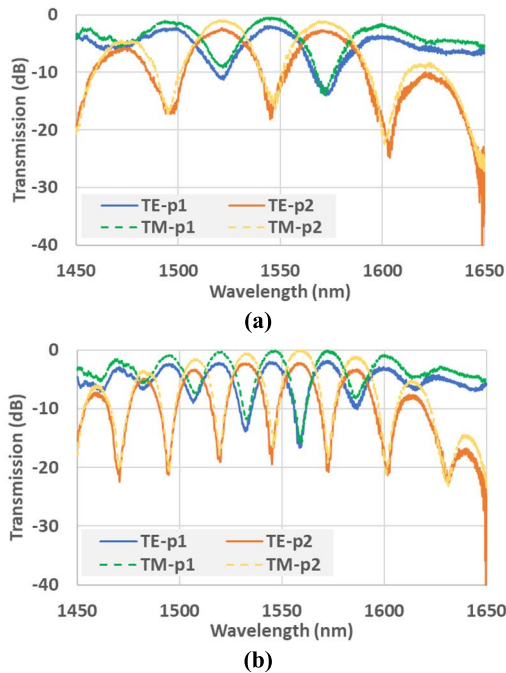


Fig. 7. Measured transmission spectrum of the fabricated PR MZI devices with the wavelength spacing of (a) 26 nm, (b) 13 nm.

Fig. 7 is the measured transmission spectra of TE and TM polarizations, for wavelength spacing of (a) 26 nm and (b) 13 nm, showing a good match in terms of the operating wavelengths between both polarizations. In general, the finer the wavelength spacing gets to be, the more difficult it becomes to achieve PI operation. From Fig. 7, even when the wavelength spacing becomes finer, PI operation is achieved. Observed PDL is about 2 dB, which can be explained as below; in the reference waveguide, the polarization of the output signal is identical to that of the input signal, while in the PR device, output polarization is converted to the orthogonal one to the input signal. Thus, if there is any PDL in the coupling between SSC and the lens facet fiber, the coupling loss calibration results in imperfect. As a result of verifying the PDL of fabricated SSC, PDL of 1.0-2.0 dB occurred as shown in Fig. 8, which could be a major factor for the PDL of PR MZI. The device loss increases at the wavelength regions shorter than 1500 nm or longer than 1600 nm due to the wavelength dependence of mode converters (Fig. 3). Because PBS1 is a normal directional coupler, it has a wavelength dependence of the coupling strength as the observed wavelength is leaving

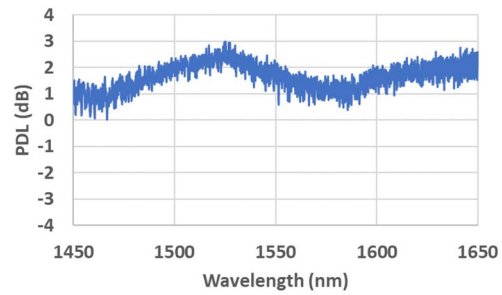


Fig. 8. Measured PDL of the coupling between SSC and the lensed fiber. Positive sign means the transmission of TE is greater than that of TM.

from the center wavelength of 1550 nm for especially TM polarization.

IV. CONCLUSION

We designed and fabricated polarization rotating (PR) Mach Zehnder interferometer (MZI) devices and experimentally verified its spectrum characteristics. PR MZI device was composed of mode converters, multimode directional couplers and PR rib waveguides. Due to the mode conversion between TE first order mode (TE₁) and TM fundamental mode (TM₀), the optical phase mismatch between them can be compensated, which means the degree of achievement of “polarization independence” is not affected by the process error. Device size was about $600 \times 120 \mu\text{m}^2$, not much larger than that of single polarized one. That means our PR MZI device has space cost merit comparing with the conventional polarization diversity scheme that requires twice the number of MZI devices designed for each polarization. The operation wavelength shows good matching between TE and TM polarizations due to the mode complementary relationship of TE₁ and TM₀.

REFERENCES

- [1] T. Tsuchizawa et al., “Microphotonic devices based on silicon micro-fabrication technology,” *IEEE J. Sel. Topics Quantum Electron.*, vol. 11, no. 1, pp. 232–240, Jan. 2005.
- [2] A. Alduino, “Demonstration of a high speed 4-channel integrated silicon photonics WDM link with hybrid silicon lasers,” in *Proc. IEEE Hot Chips Symp. (HCS)*, Aug. 2010, pp. 1–29.
- [3] Q. Wang and S. He, “Optimal design of planar wavelength circuits based on Mach–Zehnder interferometers and their cascaded forms,” *J. Lightw. Technol.*, vol. 23, no. 3, pp. 1284–1290, Mar. 2005.
- [4] S.-H. Jeong, “Broadband 1×8 channel silicon-nanowire-waveguide WDM filter based on point-symmetric Mach–Zehnder interferometric optical couplers in the O-band spectral regime,” *OSA Continuum*, vol. 2, no. 12, p. 3564, Dec. 2019.
- [5] H. Fukuda, K. Yamada, T. Tsuchizawa, T. Watanabe, H. Shinjima, and S.-I. Itabashi, “Polarization beam splitter and rotator for polarization-independent silicon photonic circuit,” in *Proc. 4th IEEE Int. Conf. Group IV Photon.*, Sep. 2007, pp. 19–21.
- [6] D. Y. Lee et al., “Error-free operation of a polarization-insensitive $4 \lambda \times 25$ Gbps silicon photonic WDM receiver with closed-loop thermal stabilization of Si microrings,” *Opt. Exp.*, vol. 24, no. 12, pp. 13204–13209, Jun. 2016.
- [7] Y. Onawa, H. Okayama, D. Shimura, H. Yaegashi, H. Sasaki, and M. Kashima, “Multimode-based polarization independent WDM devices using different order modes for TE and TM polarizations,” *Opt. Exp.*, vol. 28, no. 26, pp. 39227–39240, Dec. 2020.
- [8] Y. Shoji et al., “Simple spot-size converter with narrow waveguide for silicon wire circuits,” in *Proc. Microoptics Conf.*, Tokyo, Japan, Oct. 2009, pp. 25–28.